A kinetic theory of homogeneous bubble nucleation

Vincent K. Shen and Pablo G. Debenedetti[a)]
Department of Chemical Engineering, Princeton University, Princeton, New Jersey 08544

(Received 20 September 2002; accepted 14 October 2002)

We present a kinetic theory of homogeneous bubble nucleation based on explicit calculation of the single-molecule evaporation and condensation rates as a function of the size of the vapor embryo. The surface condensation rate is calculated from the kinetic theory of gases, and the surface evaporation rate is related to the rate of escape of molecules from a potential well in the field established by the liquid–vapor interface. Equality of these rates corresponds naturally to the critical bubble. While the interface plays a crucial role in this respect, the kinetic nucleation theory does not invoke an explicit surface tension. The nucleation rate is derived from a population balance and depends only on the ratio of the evaporation to condensation rates. In contrast to classical theory, a nontrivial trend captured by the present theory is the increase in nucleation rate with decreasing temperature at fixed degree of metastability. Comparison with classical nucleation theory reveals markedly different supersaturation dependencies of the nucleation rate, while the predicted sizes of the critical bubble are in good agreement. © *2003 American Institute of Physics.*
[DOI: 10.1063/1.1526836]

I. INTRODUCTION

In spite of their importance and ubiquity, significant gaps persist in our understanding of the thermodynamics and kinetics of metastable liquids. Consequently, fundamental knowledge of technologically important phenomena ranging from crystallization and glass formation[1] to cavitation[2] and explosive boiling[3] remains incomplete. The study of metastability in liquids can be approached either from an equilibrium (statistical mechanical) or from a kinetic viewpoint. Rigorous statistical mechanical studies of metastable liquids inevitably involve the imposition of constraints that maintain the liquid's state of metastability by preventing it from transforming into the stable phase.[1,4–8] Kinetic approaches, on the other hand, focus on the actual mechanism and rate by which metastable liquids undergo phase transitions. This paper adopts the latter approach to study bubble nucleation in superheated liquids.

Nucleation of vapor bubbles in a metastable (superheated) liquid is an important yet incompletely understood phenomenon that plays a key role in a variety of technically relevant situations, including cavitation,[2] cavitation erosion,[9,10] explosive boiling,[3,11,12] sonoluminescence,[13] and sonochemistry.[14] Knowledge of this mechanism at the molecular level is also key to reconciling major discrepancies between theoretically predicted and observed limits of liquid superheating[15,16] and tension.[2,17,18] In practical situations, bubble formation is facilitated by the presence of an external surface which usually takes the form of dissolved or suspended impurities or the walls containing the metastable liquid. This is referred to as heterogeneous bubble nucleation. In the absence of such heterogeneities, formation of the vapor phase must take place entirely within the bulk metastable liquid, and this is called homogeneous bubble nucleation. While the conditions required for observing truly homogeneous nucleation seem far removed from those encountered in practice, homogeneous bubble nucleation can nevertheless be attained in carefully controlled experiments.[1] It represents a fundamental and reproducible relaxation mechanism characteristic of the liquid state itself, and it is on this phenomenon that we focus our attention in this work.

Here, we present a kinetic theory of homogeneous bubble nucleation based on the original ideas of Ruckenstein and co-workers,[19–26] who proposed a useful and insightful kinetic approach to nucleation. We apply our theory to the superheated Lennard-Jones fluid. The theory has two important features. The first is the explicit calculation of the rate of escape of molecules from a potential energy well established by the interface between the emerging vapor embryo and the metastable liquid, and the second is the formulation of a population balance based on the *excess* number in the embryo, defined as the difference between the number of molecules in the embryo and number of molecules in a region of the same size occupied by the bulk metastable liquid. The theory predicts, as it should, that the nucleation rate increases with superheating (i.e., supersaturation) at constant temperature while the size of the critical bubble decreases. An important nontrivial trend captured by the theory is the increase of the nucleation rate with decreasing temperature at fixed degree of metastability, a result that classical theory fails to predict. In addition, the predictions of the theory adhere to the thermodynamic scaling laws originally proposed by McGraw and Laaksonen[27] for droplet nucleation, and recently extended by Shen and Debenedetti[28] for bubble formation. The format of this paper is as follows. In Sec. II, we provide a brief overview of theoretical approaches to the study of homogeneous bubble nucleation. In Sec. III, the theoretical formalism is presented. Results and discussion are presented in Sec. IV. Finally, conclusions are presented in Sec. V.

a)Electronic mail: pdebene@princeton.edu

II. HOMOGENEOUS BUBBLE NUCLEATION: THEORETICAL APPROACHES

While homogeneous bubble nucleation has been recognized for over a century as the fundamental mechanism by which a superheated liquid devoid of impurities transforms into a stable vapor,[29] a rigorous theory for this phenomenon does not exist. Before presenting our approach, we review important developments in the theoretical study of bubble formation. This discussion will introduce some of the subtle and difficult questions involved.

Thermodynamically, the reversible work of forming an embryo of a new phase from within a pre-existing metastable one comprises two contributions. The first is associated with the cost of creating an interface and is therefore proportional to the surface area of the developing embryo. The second is related to the thermodynamic driving force tending to lower the overall free energy of the system by forming the stable phase, and is therefore proportional to the embryo volume. The competition between these two contributions gives rise to a critically sized embryo such that larger nuclei grow spontaneously into the stable phase while smaller embryos shrink spontaneously and disappear into the metastable surroundings. In general, the steady-state rate of nucleation J_{SS}, that is to say the number of critical nuclei formed per unit time and volume, can be written in Arrhenius form

$$J_{SS}=A\cdot\exp\left(\frac{-W^*}{k_BT}\right), \tag{1}$$

where A is a kinetic frequency factor that in general depends weakly on temperature, T is the temperature, k_B is Boltzmann's constant, and W^* is the nucleation free-energy barrier, or the reversible work needed to form a critical nucleus. While Eq. (1) is consistent with the activated dynamics associated with the above thermodynamic arguments, it can also be derived from a kinetically based population or mass balance describing the change in the number of embryos or clusters of a certain size with respect to time in terms of single-molecule evaporation and condensation events at the surface. Because the rates of these molecular surface processes, in particular the evaporation rate from a curved surface, are generally unknown, equilibrium arguments are usually invoked to link the unknown evaporation rate to the condensation rate, which is known from the kinetic theory of gases. The resulting expression for the rate of nucleation thus becomes a function of the equilibrium distribution of embryos in the metastable phase. The equilibrium concentration of an embryo of a given size is in turn related through statistical mechanical arguments to the Boltzmann factor of the reversible work associated with its formation. Notice that this approach transforms the kinetic description of nucleation into a thermodynamic one, where the free-energy barrier is the crucial quantity controlling the rate. The theory presented in this paper addresses this underlying problem directly, by calculating explicitly the rates of evaporation and condensation at the embryo's surface.

Most theoretical treatments of nucleation have focused on the thermodynamic calculation of the free-energy barrier height W^*, an approach that is in principle justified in light of the sharp dependence of the nucleation rate on this quantity. In so-called classical nucleation theory (CNT),[1,30,31] which has historically provided the canonical description of nucleation phenomena, it is assumed that pre-critical and critical embryos are macroscopic and uniform objects possessing the properties of the thermodynamically stable phase. Within the classical framework, the free-energy barrier height for homogeneous bubble nucleation is given by

$$W^*_{\mathrm{CNT}}=\frac{16\pi\gamma^3}{3(P'-P)^2}, \tag{2}$$

where P' is the pressure within the critical bubble, P is the pressure of the bulk liquid, and γ is the surface tension, which is assumed to be the same as that for a planar liquid–vapor interface. The predictions of the classical theory are only qualitatively correct. Both the free-energy barrier and the size of the critical bubble are rightly predicted to diverge at phase coexistence, and to decrease as the extent of penetration into the metastable region increases. However, CNT applies macroscopic thermodynamics to microscopic objects (i.e., pre-critical and critical nuclei). Accordingly, an important deficiency of this theory is its inability to predict loss of stability, that is to say a vanishing free-energy barrier. This shortcoming is directly related to the use of macroscopic thermodynamic arguments,[1] in particular a size-independent surface tension. Yet, despite its limitations, classical nucleation theory nevertheless provides a basic reference with which to compare new theories and interpret experimental measurements.

In contrast to the classical theory's continuum viewpoint, statistical mechanical approaches address the molecular-level description of nucleation. While most such efforts have centered on droplet formation and crystallization, the theoretical difficulties encountered are quite general in nature, and they are directly related to the problem of identifying the emerging embryo at the molecular level. An underlying construct in statistical mechanical approaches to nucleation is the embryo of the incipient thermodynamically stable phase or the so-called "physical cluster."[32–34] The rationale behind the concept of a physically consistent cluster is to provide a rigorous microscopic definition of an embryo of the emerging phase. This is necessary in order to enumerate those configurations that contribute to the system's partition function, and therefore its free energy, which in turn enables the calculation of the reversible work of forming a critical nucleus. To illustrate the difficulties involved, consider the simplest case of droplet formation. In this situation, the intuitive picture of an incipient liquid droplet forming within a supercooled vapor is easy to envision, but identifying or characterizing such an object given a snapshot of the metastable system is not at all straightforward. Similar difficulties exist in the study of crystallization in a supercooled liquid. In the case of crystal nucleation, such difficulties are compounded by observations from simulation[35,36] and experiment[37,38] which indicate that the crystal structure of the critical nucleus is not necessarily that of the bulk stable phase. For the case of bubble formation, a microscopic picture of an emerging vapor embryo, that is to say one that is able to identify unambiguously which molecules belong to the bubble and which do not, is

not easy to envision. Such a picture must reconcile the fact that a bubble is composed mostly of empty space, yet it also contains mass. The corresponding difficulty in assigning molecules to a bubble renders the microscopic study of bubble nucleation particularly challenging.

Nevertheless, because a bubble is composed largely of empty space, especially at sufficiently low temperatures, a significant contribution to the energetics of forming a critical bubble is associated with the work of forming a cavity. While cavity formation in stable liquids has been addressed in the context of solvation and protein folding,[39–43] comparatively less attention has been paid to it in the context of bubble nucleation in metastable liquids.[6,8] Recently, Punnathanam and Corti[44] have demonstrated by computer simulation that cavities exceeding a critical size are able to destabilize the Lennard-Jones liquid under tension, causing it to undergo a macroscopic liquid-to-vapor phase transition. However, a vapor bubble is not composed entirely of empty space; it contains a small number of molecules that cannot simply be ignored. For example, in bulk liquid helium, it has been observed experimentally that bubbles preferentially form around electrons, He atoms, or He_2 molecules.[45,46] Thus, an open question is how the presence of particles in the cavity region influences the overall energetics of bubble formation.

Density-functional theory (DFT) approaches to homogeneous nucleation, pioneered by Oxtoby and co-workers,[47–50] rely on the description of a metastable system in terms of a spatially varying density field. Provided that the system can be coarse grained, the density field corresponding to the critical nucleus is a saddle point in functional space (i.e., the space defined by all possible density fields). Most DFT studies have focused on crystallization[47,48,51,52] and droplet formation;[49,50,53] comparatively less attention has been paid to bubble nucleation. Early DFT studies of bubble nucleation in the Lennard-Jones[50] and Yukawa[49] fluids and ^{3}He (Ref. 54) by Oxtoby and co-workers were the first to identify nonclassical nucleation effects, in particular the fact that the density at the center of the critical bubble at conditions sufficiently far removed from coexistence differs appreciably from that of the stable vapor. Recent DFT work[28] has shown that in liquids under high tension the density at the center of the critical bubble can be at least an order of magnitude greater than that of the stable vapor. It has also been shown that the DFT-predicted free-energy barrier height agrees well with classical theory in the vicinity of phase coexistence, but, improving over the classical picture, it in fact vanishes at the thermodynamic liquid spinodal.

Computer simulation has proven valuable in investigating the microscopic processes that trigger the nucleation of crystals, droplets, and bubbles. Direct simulation methods[55–63] consist of preparing a metastable system and simply evolving it in time until nucleation occurs. While this approach in principle provides dynamical information regarding the nucleation process, it is computationally inefficient because most of the time is spent simply waiting for nucleation to take place. Alternatively, biased sampling methods, namely umbrella sampling,[64–68] first introduced in a nucleation context by Frenkel and co-workers to study crystallization in the supercooled Lennard-Jones liquid,[69–71] force the metastable system to traverse the free-energy barrier reversibly along a reaction coordinate by means of a biasing potential. Such an approach relies on the choice of an appropriate order parameter. Early applications of umbrella sampling to study homogeneous bubble nucleation used global order parameters to estimate the height of the free energy barrier.[72,73] Using bulk density as the order parameter,[72] it was shown that the calculated free-energy barrier agreed well with classical theory for relatively small degrees of superheating and, in fact, vanished at the liquid spinodal. Assuming that a bubble was composed solely of empty space, the critical bubble was identified as a web-like, system-spanning cavity whose spatial extent decreased with increasing temperature. Although a global order parameter makes no assumptions about the shape or number of critical nuclei formed in the system, it is of course more desirable to use a local order parameter for such calculations because this provides an unambiguous description of the energetics of forming a single critical bubble. Unfortunately, a microscopic definition capable of identifying localized low-density regions within a metastable liquid remains lacking.

The so-called nucleation theorem, originally derived by Oxtoby and Kashchiev[74] using general thermodynamic arguments, and recently proved on a microscopic basis by Bowles *et al.*,[75,76] is a general result relating the supersaturation dependence of the free-energy barrier to the size of the critical nucleus. This provides an accurate means of determining the number of molecules in the critical nucleus from measured nucleation rates, assuming an Arrhenius-type expression for the nucleation rate to calculate the barrier height. Using the nucleation theorem, McGraw and Laaksonnen[27] derived general thermodynamic scaling laws for droplet nucleation relating how the free-energy barrier and size of the critical nucleus should scale with supersaturation. Subsequently, Talanquer[77] evaluated the constants in the above scaling relations by exploiting the fact that the free-energy barrier vanishes at the spinodal. The scaling relationships were verified against DFT predictions and limited experimental data for droplet formation.[27,77] Recently, we extended these relations to bubble formation and verified them numerically using DFT calculations for homogeneous bubble nucleation in the stretched Lennard-Jones liquid.[28] The value of scaling relationships lies in their ability to validate theories of nucleation and correlate experimental data, as we demonstrate in Sec. IV.

While the energetics of bubble formation represents an important aspect of nucleation in superheated liquids, it is important to emphasize that nucleation is an inherently kinetic phenomenon. Attempts to address the problem of homogeneous nucleation kinetically are relatively recent.[78–80] Noteworthy among these approaches is the work of Ruckenstein and co-workers.[19–26] The key insight provided by this important body of work is to formulate the calculation of escape rates in terms of a potential well in the immediate vicinity of the interface separating the emerging embryo from its metastable surroundings. The mean passage time of molecules across this potential barrier is directly related to the surface evaporation rate, and the steady-state nucleation

rate can be determined from a population balance using the calculated rates of accretion and depletion. Early applications of this kinetic approach addressed homogeneous droplet formation[21,22,24] and crystallization[19,20,26] in the van der Waals fluid. Subsequent extension to crystallization in colloidal systems[81] reproduced experimentally observed nucleation rate behavior, in particular a rate maximum as a function of density or volume fraction. The kinetic theory presented in this paper is based on the approach introduced by Ruckenstein and co-workers[19,20,26] and is discussed in detail in the following section.

III. THEORETICAL FRAMEWORK

In this section, the theoretical framework of the kinetic theory for homogeneous bubble nucleation is presented. The general outline of this section is as follows. First, the population balance for homogeneous bubble nucleation is reformulated and used to derive an expression for the steady-state nucleation rate. This initial step clearly demonstrates the inherent kinetic nature of nucleation phenomena, in particular the need for knowledge of the surface condensation and evaporation rates. Second, we show that there exists a potential field established by the liquid–vapor interface separating the emerging vapor bubble from the metastable surroundings. The key feature of this field is a potential energy minimum in the immediate vicinity of the interface, and it is precisely this energy minimum that is exploited to calculate the surface evaporation rate. In addition, it will be shown that the dependence of the depth of this minimum on embryo size plays a key role in the physics of embryo growth and collapse. Last, we derive the expressions needed for computing the escape rate from this potential energy well by posing the calculation in terms of a barrier-escape problem.

A. Steady-state nucleation rate

The key quantity of interest in nucleation theory is the steady-state nucleation rate J_{SS}, that is to say the rate of formation of critical nuclei per unit volume. In this subsection, we derive an expression for the bubble nucleation rate using a population balance. It is useful first to write the population balance for droplet formation, a phenomenon for which a clear physical picture is more easily invoked. A liquid-like embryo can be described in terms of the number of molecules it contains, j. The population balance for droplet nucleation reads

$$\frac{d}{dt}f_j(t)=\beta_{j-1}f_{j-1}(t)-\alpha_j f_j(t)-\beta_j f_j(t)+\alpha_{j+1}f_{j+1}(t), \tag{3}$$

where $f_j(t)$ is the concentration of embryos containing j molecules at time t, α_j is the evaporation rate of molecules from the surface of an embryo of size j, and β_j is the condensation rate of molecules onto the surface of an embryo of size j. The α and β quantities have units of reciprocal time, and already include the appropriate multiplicative factor proportional to the cluster's surface area. While the population balance is performed most naturally using the number of molecules j in an embryo as the relevant variable, it is instructive (and important for what follows) to use the excess number instead. The excess number in an embryo, Δn, is defined as the difference between the number of molecules actually in the embryo and the number of molecules present in the embryo region if it were occupied by the uniform metastable medium. The use of this variable is suggested by the nucleation theorem.[74] In its most general form, this rigorous thermodynamic result naturally relates the partial derivative of the free-energy barrier with respect to chemical potential (supersaturation) to the excess number in the critical nucleus. Note that in the case of droplet nucleation, and for the usual situation in which the density of the supercooled vapor is much less than that of the emerging droplet, the number of molecules in the embryo and the excess number are virtually identical. However, for the case of bubble nucleation, the two quantities differ greatly in magnitude, and in fact have different signs. In the present theory for homogeneous bubble nucleation, we derive the steady-state nucleation rate based on a population balance using the excess number Δn as the appropriate descriptor of the emerging vapor bubble. In other words, we identify a bubble by the difference between the actual number of molecules that constitute it and the number of molecules that would occupy the same region of space at a density equal to that of the bulk metastable liquid. For convenience, we let i denote $-\Delta n$ so as to work with positive quantities. Because vapor bubbles grow by surface evaporation and decay by surface condensation,[1] the bubble population balance differs from that for droplet nucleation and is given by the following expression:

$$\frac{d}{dt}f_i(t)=\alpha_{i-1}f_{i-1}(t)-\beta_i f_i(t)-\alpha_i f_i(t)+\beta_{i+1}f_{i+1}(t), \tag{4}$$

where $f_i(t)$ denotes the concentration of i-embryos at time t in the metastable liquid, α_i is the evaporation of rate from the surface of an i embryo, and β_i is the corresponding condensation rate. The flux $J_i(t)$ is defined to be the rate per unit volume at which $(i-1)$-embryos become i-embryos

$$J_i(t)=\alpha_{i-1}f_{i-1}(t)-\beta_i f_i(t). \tag{5}$$

At this point, it is convenient to invoke an equilibrium distribution of embryos f_i^{eq}. Contrary to what is done in classical nucleation theory, however, the equilibrium distribution is not invoked as a means for calculating the unknown quantity α_i from the known quantity β_i. Instead, the equilibrium embryo distribution enters the theory only as a physically consistent boundary condition for the calculation of the nucleation rate. An equilibrium distribution of embryos f_i^{eq} must satisfy the condition $J_i(t)=0$ for all i and t. It therefore follows that

$$\alpha_{i-1}f_{i-1}^{\mathrm{eq}}=\beta_i f_i^{\mathrm{eq}}. \tag{6}$$

For notational convenience, let $F_i(t)$ be the ratio of the actual to equilibrium concentration of i-embryos

$$F_i(t)=\frac{f_i(t)}{f_i^{\mathrm{eq}}}. \tag{7}$$

Note that i is a discrete variable. For mathematical purposes, it is convenient to consider the continuum limit. There are

various ways to convert the discrete population balance equation into a continuous one.[23,82] Here, we follow the approach of Frenkel[83] and Zeldovich.[31] Substituting Eqs. (6) and (7) into Eq. (4), the population balance becomes

$$\frac{\partial}{\partial t}f(g,t)=\beta(g)f^{\mathrm{eq}}(g)[F(g-1,t)-F(g,t)] + \beta(g+1)f^{\mathrm{eq}}(g+1)[F(g+1,t)-F(g,t)], \tag{8}$$

where g is the continuous analog of the discrete variable i. Expanding the terms $F(g-1,t)$, $\beta(g+1)$, $f^{\mathrm{eq}}(g+1)$, and $F(g+1,t)$ about g and retaining terms only up to second order, Eq. (8) can be converted into a partial differential equation

$$\frac{\partial}{\partial t}f(g,t)=\frac{\partial}{\partial g}\left[\beta(g)f^{\mathrm{eq}}(g)\frac{\partial}{\partial g}F(g,t)\right]. \tag{9}$$

Note that this resembles a diffusion equation for which the flux $J(g,t)$ is

$$J(g,t)=-\beta(g)f^{\mathrm{eq}}(g)\frac{\partial}{\partial g}F(g,t). \tag{10}$$

At steady state, the distribution of embryo sizes is time invariant, as is the nucleation rate. As a result, the steady-state nucleation rate is also necessarily independent of g and therefore becomes

$$J_{SS}=-\beta(g)f^{\mathrm{eq}}(g)\frac{\partial}{\partial g}F(g). \tag{11}$$

It is reasonable to expect that the concentration of embryos beyond some sufficiently large size, denoted by G, be vanishingly small. Otherwise, a significant portion of the vapor phase will have already formed. Thus, one can write, for sufficiently large G

$$F(G)=0. \tag{12}$$

Furthermore, at the other extreme, an embryo of excess size $g=0$ is indistinguishable from a liquid monomer and therefore the concentration of these particular embryos is the same as the concentration of liquid monomers. Thus, for $g=0$

$$F(0)=1. \tag{13}$$

Using Eq. (12) as a boundary condition, Eq. (11) can be solved for $F(g)$, to yield

$$F(g)=J_{SS}\left[\int_0^G dx\frac{1}{\beta(x)f^{\mathrm{eq}}(x)}-\int_0^g dx\frac{1}{\beta(x)f^{\mathrm{eq}}(x)}\right]. \tag{14}$$

Finally, using Eq. (13), an expression for the steady-state nucleation rate can be derived

$$J_{SS}=\frac{1}{\int_0^G (dx/[\beta(x)f^{\mathrm{eq}}(x)])}. \tag{15}$$

The equilibrium distribution of embryos $f^{\mathrm{eq}}(x)$ can be determined from Eq. (6)

$$f^{\mathrm{eq}}(g)=f^{\mathrm{eq}}(0)\prod_{j=1}^{g}\frac{\alpha_{j-1}}{\beta_j}. \tag{16}$$

Inserting this into Eq. (15) and letting $G\to\infty$, J_{SS} reduces to

$$J_{SS}=\frac{\beta(0)f(0)}{\int_0^\infty dx\cdot\exp[\Sigma_{j=1}^{x-1}\ln(\beta_j/\alpha_j)]}, \tag{17}$$

where $f(0)$ is just the number density of the bulk metastable liquid since an embryo whose number excess is zero is simply a liquid monomer. It follows that $\beta(0)$ is the average collision rate of single molecule in the liquid medium. Notice that the steady-state nucleation rate depends explicitly on the surface evaporation and condensation rates as a function of embryo size, which are purely kinetic quantities. The equilibrium embryo distribution enters the theory exclusively through the boundary conditions, Eqs. (12) and (13). While the condensation or arrival rate can be reasonably estimated using the kinetic theory of gases, the main difficulty lies in how to determine the evaporation or escape rate. We address this problem below.

B. Potential energy field

The evaporation of molecules from a surface can be viewed as an escape from a potential energy well. Within the context of bubble formation, the conceptual situation of interest consists of a spherical vapor embryo of radius R and uniform density ρ_V situated in a metastable liquid of density ρ_L. Molecules are assumed to interact via a spherically symmetric, pairwise additive potential $u(d)$ where d denotes the distance between pairs of molecules. In this work, we use the Lennard-Jones potential, which provides a realistic description of interactions in monatomic liquids. It is given by

$$u_{\mathrm{LJ}}(d)=4\varepsilon\left[\left(\frac{\sigma}{d}\right)^{12}-\left(\frac{\sigma}{d}\right)^{6}\right], \tag{18}$$

where ε is the well depth, and σ is the interatomic distance at which the potential energy is zero. Consider a molecule in the vapor embryo located a distance q from the interface. In order to calculate the potential energy felt by this molecule, consider a plane defined by a great circle that contains the centers of the molecule and the vapor bubble as shown in Fig. 1. Any great circle whose diameter is the line joining the molecule of interest and the bubble's center can be used for this calculation. An infinite number of such circles exist, and it is not necessary to specify any one in particular. Using a Cartesian coordinate system, let the origin coincide with the center of the molecule of interest, where the y axis is defined by the unit vector pointing from the molecule to the center of the bubble and the x axis is the unit vector perpendicular to the y axis lying on the above-defined plane. In this coordinate system, it naturally follows that the equation of the great circle is $x^2+[y-(R-q)]^2=R^2$. Note that this two-dimensional picture is based on the existence of cylindrical symmetry about the y axis, which allows us to perform the full three-dimensional calculation straightforwardly. Assuming that $\rho_L\gg\rho_V$, the potential energy $\phi(q;R)$ felt by this molecule for an arbitrary spherically symmetric potential $u(d)$ is given by

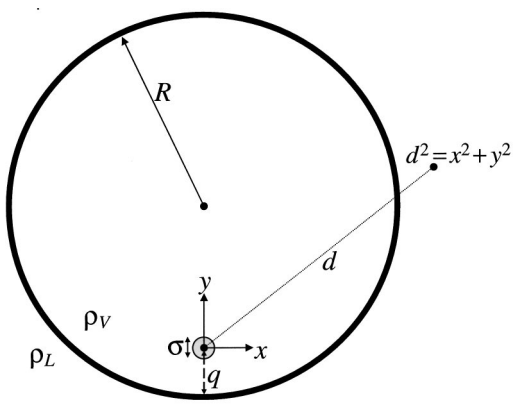

FIG. 1. Schematic setup for calculating the potential energy felt by a molecule located a distance q from the surface of a spherical bubble of radius R and density ρ_V situated in a liquid of density ρ_L. What is shown is a plane defined by a great circle that contains the molecule and embryo centers. The origin of a Cartesian coordinate system in this plane is fixed at the molecule's center, where the y axis is defined as the unit vector pointing towards the center of the embryo and the x axis is the unit vector perpendicular to the y axis lying on the above-defined plane. Note that in this two-dimensional representation there exists cylindrical symmetry about the y axis.

$$\phi(q;R)=2\pi\rho_L\left[\int_{-\infty}^{-q}dy\int_0^{\infty}dx\cdot x\cdot u(d)+\int_{-q}^{2R-q}dy\int_{\sqrt{R^2-[y-(R-q)]^2}}^{\infty}dx\cdot x\cdot u(d)+\int_{2R-q}^{\infty}dy\int_0^{\infty}dx\cdot x\cdot u(d)\right], \tag{19}$$

where $d=\sqrt{x^2+y^2}$ and the factor 2π arises from exploiting cylindrical symmetry about the y axis. In Fig. 2, this potential energy field is plotted as a function of q for several values of R using the Lennard-Jones interaction potential. In all cases, there exists a minimum in potential energy at a distance $q_{\min}<\sigma$ from the interface for all embryo sizes. That $q_{\min}<\sigma$ is attributed to the fact that a molecule inside the bubble near the interfacial region feels only an attractive force acting on it from one side. This minimum can be thought to give rise to a thin shell of molecules, the escape from which determines the surface evaporation rate. Note that the well depth decreases with increasing embryo size, which has an important physical consequence. The inverse relationship between the well depth and embryo size indicates that the surface evaporation increases with embryo size. As will be shown, this effect plays a key role in determining the size of the critical bubble. As $R\to\infty$, the potential field reduces to that of an infinite, planar liquid–vapor interface. For the Lennard-Jones fluid, we have verified analytically that Eq. (19) reduces to the familiar inverse 9–3 power potential[84] in the limit as $R\to\infty$.

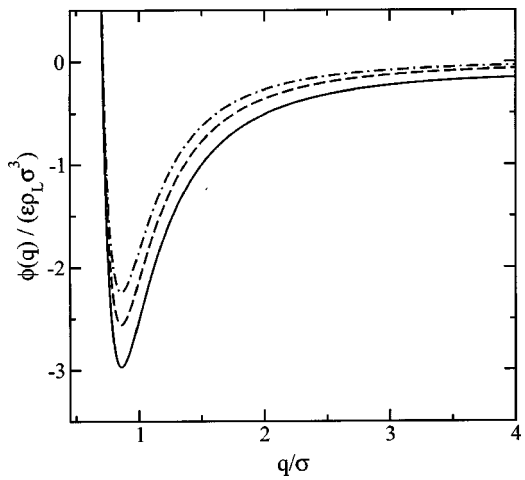

FIG. 2. The dimensionless potential energy field plotted as a function of distance from the interface q using the Lennard-Jones potential for several embryo sizes, $R=5\sigma$ (—), 10σ (– – –), and 100σ (— — —).

While the evaporation rate calculation is posed in terms of a barrier-crossing problem, the potential calculated through Eq. (19) and plotted in Fig. 2 does not exhibit a maximum as a function of q, but instead increases monotonically toward the center of the bubble. While there exists a relative maximum at the center of the embryo, $q=R$, it is unreasonable to require a molecule to reach the center of the embryo for it to be considered "dissociated" because extension of this explicit barrier-crossing requirement to the planar liquid–vapor interface where $R\to\infty$ leads to the unphysical conclusion that only molecules infinitely far away from the interface on the low-density side can be considered dissociated, or belonging to the vapor phase. Although the lack of an explicit potential energy barrier renders the definition of a dissociated molecule somewhat arbitrary, we can construct such a definition rationally based on the following observations of the potential field (Fig. 2). It can be seen that most of the steep energy change occurs in the immediate vicinity of the potential energy minimum, and it is in this region where the molecule must do most of the work to escape the influence of the field. Beyond some distance from the interface, $q_{\rm dis}$, the potential field is relatively flat and therefore the force on the molecule is correspondingly small. Under these conditions, a molecule can be considered dissociated or having escaped from the well for all practical purposes. In more precise terms, we define $q_{\rm dis}$ as the distance at which a molecule has climbed some sufficiently large fraction ξ of the potential energy difference between that at the center of the embryo ($q=R$) and the minimum ($q=q_{\min}$). Mathematically, $q_{\rm dis}$ is defined as satisfying the following condition:

$$\phi(q_{\rm dis};R)=\xi\cdot[\phi(R;R)-\phi(q_{\min};R)]+\phi(q_{\min};R). \tag{20}$$

In what follows, it is more convenient to express the potential field as a function of radial distance from the center of the vapor embryo, r, rather than the distance from the interface, q. Using the fact that $q=R-r$, we make the following transformation:

$$\phi(q;R)\to\phi(r;R). \tag{21}$$

It naturally follows that

$$r_{\min}=R-q_{\min}, \tag{22}$$

and

$$r_{\mathrm{dis}} = R - q_{\mathrm{dis}}. \tag{23}$$

Finally, we denote by r_b the radial position at which the potential field is zero. Because of the steep repulsive force at this position, r_b corresponds physically to the closest approach to the bulk liquid for a molecule in the embryo's interior. Thus, the domain of the potential energy field of interest extends from r_{dis} to r_b, where $r_{\mathrm{dis}} < r_{\min} < r_b$.

C. Escape and arrival rates

In this subsection, we derive an expression for the mean passage time of molecules across the potential well, which is inversely related to the surface evaporation rate α, and governs the growth of vapor embryos. In addition, the standard kinetic theory[85] expression for the condensation rate β will be presented here for completeness. The molecules of interest are those that comprise the thin shell of thickness η and density ρ_{shell} that tends to form in the vicinity of the potential energy minimum. Consider now the motion of an individual molecule within the potential well region. It undergoes Brownian motion due to collisions with other molecules. The random nature of such motion is described by the well-known Fokker–Planck equation.[86] The Fokker–Planck description is simplified significantly under conditions where the velocity distribution is equilibrated (i.e., it becomes Maxwellian) on a time scale much shorter than that needed for positional equilibration. This is precisely the case when a molecule is situated in a liquid-like environment or when there is strong coupling between it and the surrounding medium. Exploiting this separation of time scales, the positional evolution of the molecule can be described by the *forward* Smoluchowski equation,[86] which takes the following form in a system possessing spherical symmetry:

$$\frac{\partial}{\partial t} p(r,t|r_0) = \frac{D}{r^2} \frac{\partial}{\partial r} \left\{ r^2 \exp\left[\frac{-\phi(r;R)}{k_B T} \right] \frac{\partial}{\partial r} \times \left[\exp\left(\frac{\phi(r;R)}{k_B T} \right) p(r,t|r_0) \right] \right\}, \tag{24}$$

where $p(r,t|r_0)$ is the probability of observing the molecule at a radial position between r and $r+dr$ at time t given that it was located at r_0 initially, $\phi(r;R)$ is the potential energy field derived in the previous section, and D is the diffusion coefficient. It is worth pointing out that we have taken the origin of the system to coincide with the center of the embryo. We are ultimately interested in the probability that a molecule located initially in the region $(r_{\mathrm{dis}} < r_0 < r_b)$ is located outside of it $(r < r_{\mathrm{dis}})$ at time t. Formally, this corresponds to knowing how the probability changes with the molecule's initial position. It is therefore more convenient to deal with the *adjoint* or *backward* Smoluchowski equation[87,88] which describes changes in $p(r,t|r_0)$ with respect to the initial position, r_0. In a system possessing spherical symmetry, the *backward* Smoluchowski equation reads

$$\frac{\partial}{\partial t} p(r,t|r_0) = \frac{D}{r_0^2} \exp\left[\frac{\phi(r_0;R)}{k_B T} \right] \frac{\partial}{\partial r_0} \times \left\{ r_0^2 \exp\left[\frac{-\phi(r_0;R)}{k_B T} \right] \frac{\partial}{\partial r_0} p(r,t|r_0) \right\}. \tag{25}$$

As shown in Appendix A, the dissociation or escape time is given as a function of initial position $\tau(r_0;R)$ by the expression

$$\tau(r_0;R) = \int_{r_{\mathrm{dis}}}^{r_0} dy \cdot \frac{\exp\left[\frac{\phi(y;R)}{k_B T} \right]}{y^2} \int_y^{r_b} dx \cdot \frac{x^2}{D} \cdot \exp\left[\frac{-\phi(x;R)}{k_B T} \right]. \tag{26}$$

The average dissociation time, or the mean passage time, $\theta(R)$, is simply an average over all possible initial positions weighted by their Boltzmann factors

$$\theta(R) = \frac{1}{Z} \int_{r_{\mathrm{dis}}}^{r_b} dr_0 \cdot r_0^2 \cdot \exp\left[\frac{-\phi(r_0;R)}{k_B T} \right] \cdot \tau(r_0;R), \tag{27}$$

where Z is the partition coefficient for a molecule in a potential energy field and is given by

$$Z = \int_{r_{\mathrm{dis}}}^{r_b} dr_0 \cdot r_0^2 \cdot \exp\left[\frac{-\phi(r_0;R)}{k_B T} \right]. \tag{28}$$

Note that the mean passage time is a function of embryo size. The surface evaporation rate $\alpha(R)$ is defined as the total number of molecules N_{shell} in the spherical shell divided by the mean passage time $\theta(R)$

$$\alpha(R) = \frac{N_{\mathrm{shell}}}{\theta(R)}. \tag{29}$$

The number of molecules in the shell, N_{shell}, is

$$N_{\mathrm{shell}} = 4\pi R^2 \eta \rho_{\mathrm{shell}}, \tag{30}$$

where η is the thickness of the shell, and ρ_{shell} is its number density. Thus, the surface evaporation rate is

$$\alpha(R) = \frac{4\pi R^2 \eta \rho_{\mathrm{shell}}}{\theta(R)}. \tag{31}$$

Competing against the escape of molecules from the surface is the arrival of molecules from the interior of the vapor bubble to its surface. Note that in the case of bubble formation, vapor bubbles shrink by condensation. For simplicity, we assume that the vapor contained in the bubble behaves ideally. From the kinetic theory of gases,[85] the arrival or condensation rate of molecules, β, is simply

$$\beta(R) = \pi R^2 \langle \nu \rangle \rho_V, \tag{32}$$

where R is the radius of the vapor bubble, $\langle \nu \rangle$ is the mean velocity which is only a function of temperature, and ρ_V is the density of the vapor bubble. Note that we have implicitly assumed a sticking coefficient of unity. As in classical theory, it is assumed that the density of the vapor bubble is the same as that of the stable vapor at the given temperature.

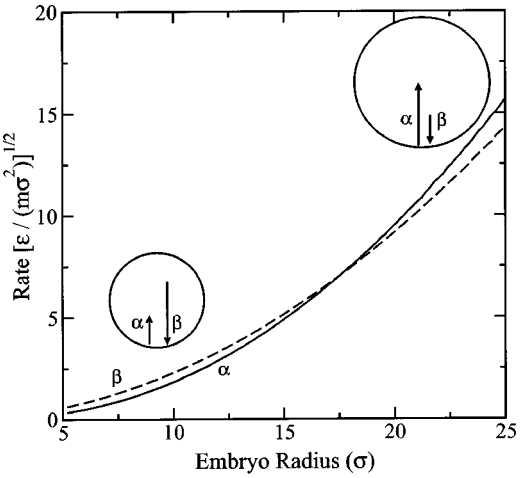

FIG. 3. The evaporation α (—) and condensation β (– – –) rates plotted as a function of embryo size R. The critical vapor bubble corresponds to the point at which the two curves cross. These calculations were performed for a liquid at $k_BT/\varepsilon = 0.80$ and $P\sigma^3/\varepsilon = -0.0126$.

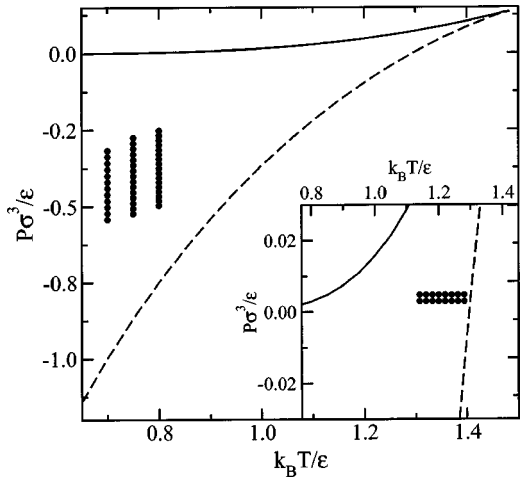

FIG. 4. Pressure–temperature projection of the liquid phase diagram for the Lennard-Jones fluid. The dark solid line is the saturation line, or binodal, and the dark dashed line is the liquid spinodal. The points (●) denote the metastable state points for which the nucleation rate calculations were performed. Notice that we have examined state points where the liquid is under tension, as well as conditions where it is heated above its boiling point (inset).

While the region of interest of the potential field extends from $r_{\rm dis}$ to r_b, it is not at all obvious what is the thickness, η, or density, $\rho_{\rm shell}$, of the shell formed by the molecules that aggregate in the vicinity of the potential well. In this work, we have assumed that these values are identical to those at saturation at the given temperature. Therefore, we take advantage of the fact that the critical bubble in the saturated liquid is infinitely large, and thus the product $\eta\rho_{\rm shell}$ can be determined from the corresponding condition of equality between condensation and evaporation rates to yield

$$\eta\rho_{\rm shell} = \frac{\langle \nu \rangle \rho_V^{\rm sat}}{4}\,\theta(R\to\infty), \tag{33}$$

where $\rho_V^{\rm sat}$ is the density of the saturated vapor. We assume that the diffusion coefficient D in the liquid does not change appreciably from its value at saturation at the same temperature. Therefore, insertion of Eq. (33) into Eq. (31) to determine the evaporation rate $\alpha(R)$ results in an expression that is independent of D.

The relative rates of evaporation $\alpha(R)$ and condensation $\beta(R)$ dictate whether the vapor embryo grows or shrinks. In Fig. 3, the escape and arrival rates are plotted as a function of embryo size for a vapor bubble in the metastable liquid. Note that both α and β increase with bubble size, but they do so at different rates. Small vapor bubbles tend to shrink and disappear into the surrounding medium because the surface evaporation rate is less than the condensation rate. Conversely, large bubbles tend to grow because the evaporation rate is larger than the condensation rate. Consequently, at some critical embryo size R^*, the evaporation and condensation rates are equal. Given the expressions for the evaporation and condensation rates as a function of size, they can be inserted into Eq. (17) to calculate the steady-state nucleation rate J_{SS}. Notice that while the liquid–vapor interface plays a crucial role in the physics, there is no explicit mention of surface tension anywhere in the kinetic theory.

IV. RESULTS AND DISCUSSION

We have applied the current kinetic theory for homogeneous bubble nucleation to the Lennard-Jones liquid under isotropic tension, as well as to higher-temperature states where superheating is caused thermally rather than mechanically. In our calculations, we use the relatively simple analytical equation of state for the Lennard-Jones fluid derived from Weeks–Chandler–Andersen perturbation theory[89] which has been used primarily in DFT approaches to homogeneous nucleation in the Lennard-Jones fluid.[28,50] Our main focus will be on the Lennard-Jones liquid at sufficiently subcritical temperatures where this equation of state is quite accurate. The liquid state points investigated in this work are shown in Fig. 4.

Because nucleation is an activated process, the steady-state rate of nucleation is usually expressed in Arrhenius form as in Eq. (1), where the main quantity governing the dynamics is the free-energy barrier height or the reversible work of forming a critically sized nucleus, W^*. As noted in Sec. II, most theoretical approaches to nucleation focus on calculating this quantity. From a thermodynamic perspective, the work of forming a critical nucleus should decrease with increasing penetration into the metastable region and vanish at some point, reflecting a crossover from activated to spontaneous phase transition dynamics. However, the nucleation rate in the current theory does not *a priori* assume an Arrhenius form. While the kinetic theory does not provide an explicit expression for the free-energy barrier, in the comparisons with the classical predictions that follow, we estimate an effective barrier height by fitting the predicted nucleation rate to an Arrhenius rate expression.

Recent DFT work on homogeneous bubble nucleation introduced the quantity $\Delta\mu/\Delta\mu_{\rm spin}$, called the degree of metastability, as a natural scaling parameter that quantifies the thermodynamic driving force.[28] The fundamental nature of this quantity was suggested by the observation that vari-

ous properties of the DFT-predicted critical bubble, such as its work of formation, size, and interfacial thickness, scaled with the degree of metastability in temperature-independent fashion. Physically, this parameter is a natural measure of the extent of penetration into the metastable region of the liquid, and is defined as

$$\frac{\Delta\mu}{\Delta\mu_{\text{spin}}}=\frac{\mu_{\text{liq}}(P,T)-\mu_{\text{sat}}(T)}{\mu_{\text{spin}}(T)-\mu_{\text{sat}}(T)}, \tag{34}$$

where $\mu_{\text{liq}}(P,T)$ is the chemical potential of the bulk metastable liquid at the given pressure P and temperature T, $\mu_{\text{sat}}(T)$ is the coexistence chemical potential at the same T, and $\mu_{\text{spin}}(T)$ is the chemical potential of the liquid at the spinodal, also at the same temperature. An equivalent interpretation of $\Delta\mu/\Delta\mu_{\text{spin}}$ is that it is simply the normalized thermodynamic driving force for nucleation. Notice that this parameter conveniently varies between zero at saturation and unity at the liquid spinodal.

The only adjustable parameter in the theory is ξ, the fraction of the energy difference between the potential well and the effective potential at the center of the embryo that a molecule must surmount before it is considered ''dissociated.'' It therefore follows that high values of ξ tend to depress the surface evaporation rate. Consequently, the predicted size of the critical nucleus increases with ξ while the nucleation rate decreases. Although the value of ξ influences the quantitative predictions of theory, it does not affect the qualitative trends. In the results that follow, we have taken $\xi=0.90$ unless noted otherwise, as this was found to yield critical bubble sizes that agreed well with classical theory predictions (within $\pm 10\%$) at the lowest temperature and highest degree of metastability investigated. This provides a convenient baseline for comparing the predictions of the classical and kinetic nucleation theories. For reference, at $k_BT/\varepsilon=0.70$, the predicted nucleation rate at $\Delta\mu/\Delta\mu_{\text{spin}}=0.390$ using a value $\xi=0.90$ is equal to that at $\Delta\mu/\Delta\mu_{\text{spin}}=0.402$ using $\xi=0.91$. This represents a modest shift in the degree of metastability.

In the current kinetic nucleation theory (KNT), the critical bubble corresponds to the condition of equality between the surface condensation and evaporation rates, $\alpha(R^*)=\beta(R^*)$. In Fig. 5, the radius of the critical bubble R^* is plotted as a function of the degree of metastability at three reduced temperatures ($k_BT/\varepsilon=0.70$, 0.75, and 0.80) for the Lennard-Jones liquid under isotropic tension. In all cases, the size of the critical bubble diverges at saturation and decreases with increasing metastability, which is consistent with intuitive expectation. In our previous work on bubble nucleation we found that the size of the DFT-predicted critical bubble scales independently of temperature with the degree of metastability.[28] The current theory instead predicts a small but non-negligible temperature dependence as can be seen from the distinct isotherms in Fig. 5. Notice that at fixed value of metastability the radius of the critical bubble increases with temperature, a trend also predicted by classical theory. A direct comparison between the current kinetic and classical nucleation (CNT) theories is made in Fig. 6, where the ratio of the KNT to CNT critical bubble radius is plotted as a function of metastability. Notice that the two theories

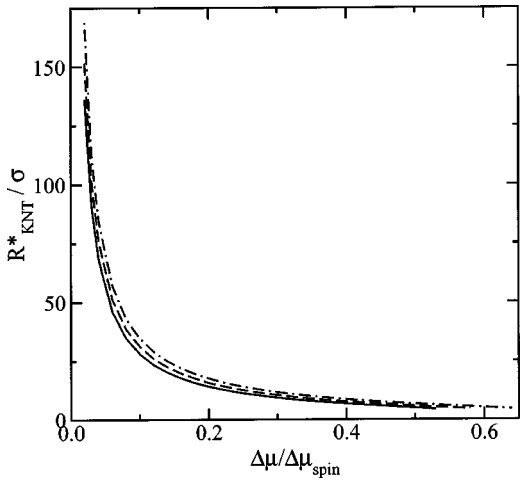

FIG. 5. The radius of the critical bubble R^* as a function of the degree of metastability $\Delta\mu/\Delta\mu_{\text{spin}}$ at three reduced temperatures, $k_BT/\varepsilon=0.70$ (—), 0.75 (– – –), and 0.80 (— – —).

predict similar values for the radius of the critical bubble (i.e., the ratio $R^*_{\text{KNT}}/R^*_{\text{CNT}}$ is not very different from unity). The observation that the ratio $R^*_{\text{KNT}}/R^*_{\text{CNT}}$ deviates from unity is actually consistent with the suggestion that the kinetically defined critical nucleus, KNT, should differ in size from the thermodynamically defined one, CNT.[90] Furthermore, notice that the discrepancy between the two predictions increases with temperature. We attribute this to the fact that at elevated temperatures, the assumption that $\rho_V \ll \rho_L$ in the kinetic theory becomes invalid. This should be anticipated because the distinction between liquid and vapor phases vanishes as the critical temperature is approached giving rise to a broad, instead of sharp, interfacial region. Therefore, the density of the embryo is no longer negligible, and the theory should not be expected to work well under these conditions.

In Fig. 7, the KNT-predicted steady-state nucleation rate $J_{SS}/\beta(0)f(0)$ is plotted against the degree of metastability for the same three temperatures in Figs. 5 and 6. Again, the

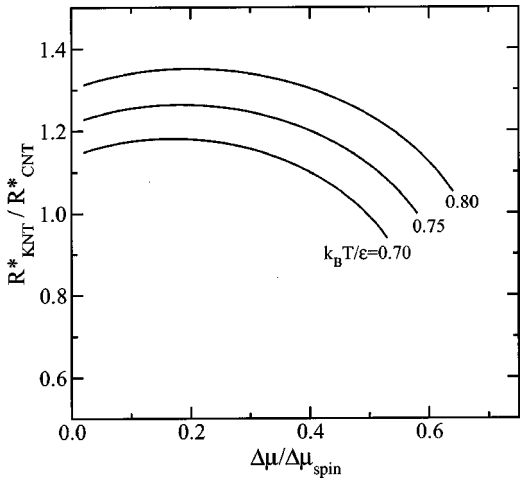

FIG. 6. Ratio of the kinetic nucleation theory (KNT) to classical nucleation theory (CNT) critical bubble radius as a function of metastability at three reduced temperatures, $k_BT/\varepsilon=0.70$, 0.75, and 0.80.

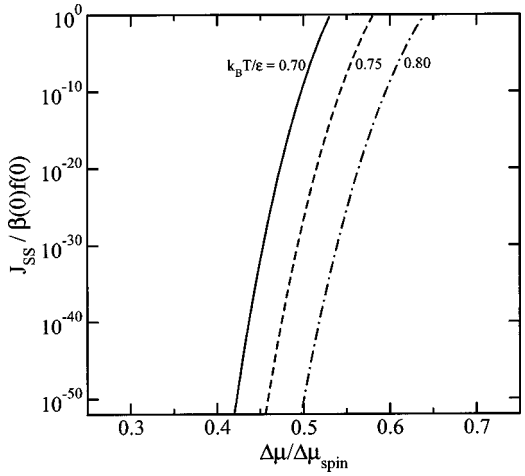

FIG. 7. Steady-state nucleation rate as predicted by the current kinetic theory as a function of metastability for a liquid under isotropic tension at three reduced temperatures, $k_BT/\varepsilon = 0.70$ (—), 0.75 (– – –), and 0.80 (– – –).

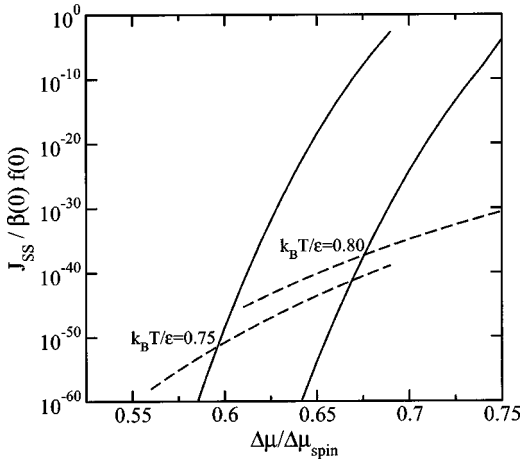

FIG. 8. Comparison of the steady-state nucleation rate predicted by KNT (—) and that predicted by CNT (– – –) at two reduced temperatures ($k_BT/\varepsilon = 0.75$, and 0.80) using ξ=0.97.

state points along each isotherm correspond to a liquid under isotropic tension (see Fig. 4). Note that the scale of the *y* axis spans 50 orders of magnitude. There are several important trends to notice in Fig. 7. First, at fixed temperature, the nucleation rate increases with metastability, that is to say with the extent of penetration into the metastable region. Second, the reduced nucleation rates reach a value of unity, indicating that an associated effective free-energy barrier vanishes. Another remarkable feature is the fact that the nucleation rate changes by many orders of magnitude over a relatively small metastability range, which is consistent with empirical observations that superheated liquids tend to undergo a sudden change from apparent stability to catastrophic boiling.[1,3,16] Finally, notice that at fixed value of metastability the nucleation rate increases with decreasing temperature. In the pressure–temperature plane (Fig. 4), lines of constant liquid metastability lie between the binodal ($\Delta\mu/\Delta\mu_{\text{spin}} = 0$) and spinodal ($\Delta\mu/\Delta\mu_{\text{spin}} = 1$) curves. Movement along a line of constant value of metastability in the direction of decreasing temperature corresponds to decreasing pressure, or increasing tension (see, e.g., the liquid spinodal in Fig. 4). One therefore expects the nucleation rate to increase with decreasing temperature at a fixed value of metastability. This is a nontrivial result in light of the fact that classical theory predicts the opposite trend, namely that the nucleation rate should decrease with decreasing temperature, due primarily to the inverse temperature dependence of the surface tension for the planar liquid–vapor interface.

A direct comparison between the nucleation rates predicted by KNT and CNT is made in Fig. 8 as a function of metastability at two reduced temperatures ($k_BT/\varepsilon = 0.75$ and 0.80) using a value of ξ=0.97. First, notice that the kinetic theory predicts a more explosive transition from apparent metastability to catastrophic boiling than does classical theory. Second, it is interesting to note that while KNT and CNT agree relatively well in predicting the size of the critical bubble, the predicted nucleation rates are dramatically different. In particular, while one expects better agreement between the two theories near coexistence, the metastability values corresponding to agreement between KNT and CNT are actually quite appreciable ($\Delta\mu/\Delta\mu_{\text{spin}} > 0.5$) and increase with temperature. However, the rate corresponding to the point at which the two theoretical curves intersect, while finite, is zero for practical purposes. Comparison of these extremely small numbers is not particularly useful. On the other hand, the discrepancy between the two theoretical rates at even higher values of metastability is substantial and is due to the fact that CNT employs a planar interfacial tension which is a gross overestimate of the true surface tension for a microscopic embryo. Consequently, classical theory always underpredicts the nucleation rate for high values of metastability [see Eqs. (1) and (2)]. We also note that the several-orders-of-magnitude difference between the rates predicted by KNT and CNT is consistent with similar kinetics-based theories of nucleation for crystals and droplets.[19–24,26] While it is desirable to discern which theory, KNT or CNT, provides a more accurate description of the actual phenomenon of homogeneous bubble nucleation, reliable experimental rate data in simple monatomic fluids, the vast majority of which is only relevant to liquids heated above their boiling points, are limited.[1,15,91,92] Furthermore, measurements in stretched liquids have been restricted to conditions corresponding to a very small degree of metastability ($\Delta\mu/\Delta\mu_{\text{spin}} = 0.02$) where both theories predict vanishing rates of bubble nucleation.[15]

An important test of the current kinetic theory is whether or not it follows the general scaling laws based on the nucleation theorem. While the McGraw–Laaksonen[27] scaling relations were originally developed specifically for droplet nucleation, recent work[28] has extended them to homogeneous bubble nucleation. In its most general form,[74] the nucleation theorem is given by

$$\frac{\partial W^*}{\partial \Delta\mu} = -\Delta n^*, \tag{35}$$

where W^* is the free-energy barrier height, $\Delta\mu$ is the chemical potential difference between the metastable and saturated liquid, and Δn^* is the excess number in the critical bubble. It

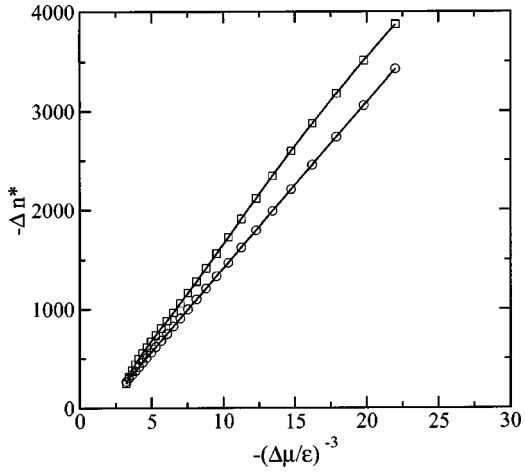

FIG. 9. Negative of the number excess in the critical bubble, $-\Delta n^*$ as a function of the nominal thermodynamic driving force, $\Delta\mu$, at $k_BT/\varepsilon = 0.70$. Squares denote the excess number calculated by a classical fit. Circles denote the excess number calculated directly from the critical nucleus condition.

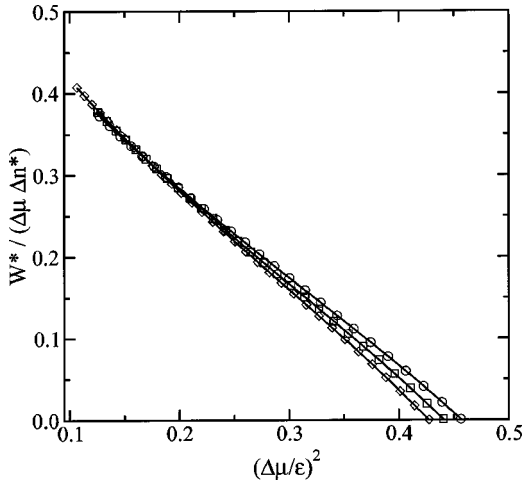

FIG. 10. Ratio of the free-energy barrier height to the product of nominal thermodynamic driving force and number excess in the critical bubble as a function of the chemical potential difference between the metastable and saturated liquid at three reduced temperatures $k_BT/\varepsilon = 0.70$ (○), 0.75 (□), and 0.80 (◇).

should be pointed that the differentiation in Eq. (35) is performed at constant temperature. Using this thermodynamic result, one can derive the following scaling relations (see Appendix B):

$$\Delta n^* = C(T)(\Delta\mu)^{-3}, \tag{36}$$

and

$$\frac{W^*}{\Delta\mu \cdot \Delta n^*} = -B(T)(\Delta\mu)^2, \tag{37}$$

where $C(T)$ and $B(T)$ are positive temperature-dependent constants. As shown in Appendix B, a key step in arriving at Eqs. (36) and (37) involves invoking a mathematical homogeneity condition.[27,28] The excess number in the critical bubble can be determined by two independent methods which can serve as verification of self-consistency. The first involves the use of the nucleation theorem, Eq. (35). While the current kinetic theory does not calculate an explicit free-energy barrier, an effective free-energy barrier height can be determined by fitting the kinetic nucleation rate to the classical form as in Eq. (1). In this case, the derivative of the effective free-energy barrier with respect to the nominal thermodynamic driving force should yield the excess number in the critical bubble. In the second method, the excess number is calculated directly from the critical nucleus condition (i.e., the equality between evaporation and condensation rates). In this case, the excess number is simply the product of the volume of the bubble and the difference between the stable vapor and metastable liquid densities. In Fig. 9, the negative of the excess number, $-\Delta n^*$, determined by the two methods is plotted as a function of $-(\Delta\mu)^{-3}$. Notice that the indirect and direct methods agree reasonably well. If the steady-state nucleation rate is instead determined using a population balance based on the actual as opposed to the excess number of molecules in the vapor embryo, this condition of self-consistency is violated. Note also that the value of $-\Delta n^*$ predicted by the indirect method is always larger than the direct one. However, the discrepancy between the two, which is attributed to the imposition of a functional form to extract the effective free-energy barrier, decreases with increasing degree of metastability. We should remark again that it has been suggested that the thermodynamically predicted number excess in the critical nucleus does not necessarily have to agree with that predicted by a kinetics-based theory.[90] Nevertheless, it is quite clear that the scaling relation in Eq. (36) holds well.

In Fig. 10, we plot the quantity $W^*/(\Delta\mu\Delta n^*)$ versus $(\Delta\mu)^2$ at three temperatures to test the scaling relation in Eq. (37), where the number excess has been calculated directly from the critical nucleus condition and the free-energy barrier has been determined indirectly from a classical fit. The isotherms are linear to a very good approximation, indicating that the scaling relation in Eq. (37) is reproduced quite well by the kinetic theory. In addition, notice that the slope of each line becomes steeper with increasing temperature, which is also consistent with the droplet nucleation results of McGraw and Laaksonen.[27] In recent work on homogeneous bubble nucleation using density-functional theory,[28] we have shown that the quantity on the left-hand side of Eq. (37) scales with the degree of metastability independently of temperature. It was also suggested, using the nucleation theorem and the homogeneity condition arguments as detailed in Appendix B, that $W^*/(\Delta\mu\Delta n^*)$ should be a quadratic function of the degree of metastability. While a quadratic functional form captured the DFT-predicted behavior reasonably well, it was evident that a higher-order functional form was required to quantitatively fit the DFT results. In Fig. 11, we plot $W^*/(\Delta\mu\Delta n^*)$ versus $(\Delta\mu/\Delta\mu_{\text{spin}})^2$ at the same three temperatures as before. Although it is obvious that there is no temperature-independent scaling behavior with respect to $\Delta\mu/\Delta\mu_{\text{spin}}$, the quantity $W^*/(\Delta\mu\Delta n^*)$ is described remarkably well by a quadratic function of the degree of metastability.

Up to this point, we have only presented nucleation rate calculations for the Lennard-Jones liquid under isotropic ten-

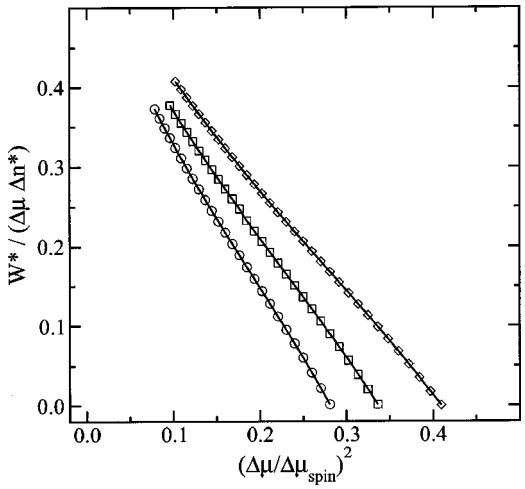

FIG. 11. Ratio of the free-energy barrier height to the product of nominal thermodynamic driving force and number excess in the critical bubble as a function the degree of metastability at three reduced temperatures $k_BT/\varepsilon = 0.70$ (○), 0.75 (□), and 0.80 (◇).

sion where the driving force for nucleation is of a mechanical origin. In many practical settings, bubble nucleation occurs in liquids that have been heated above their boiling point where the driving force is of a thermal nature and effects such as a pronounced temperature-dependent surface tension become important.[1] Recall that one of the assumptions in the kinetic theory is that the density of the stable vapor is much less than that of the metastable liquid. This assumption becomes increasingly invalid at elevated temperatures, particularly close to the critical point. Furthermore, the WCA equation of state for the Lennard-Jones liquid[89] is not very accurate at elevated temperatures, although it is particularly well-suited in describing the properties of the liquid at sufficiently subcritical temperatures. Although the use of a more sophisticated equation of state will not influence the qualitative trends that we wish to present here, some caution must be exercised in using the theory in its present form at these conditions. In Fig. 12, the steady-state nucleation rate is plotted as a function of temperature at two different pressures

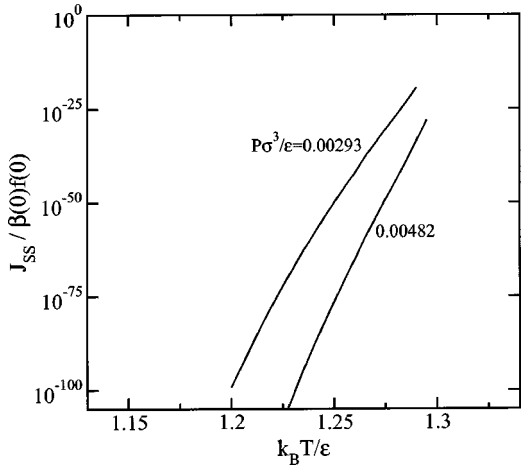

FIG. 12. Steady-state nucleation rate as a function of temperature for a liquid superheated beyond its boiling point at two different external pressures $P\sigma^3/\varepsilon = 0.002\,93$ and $0.004\,82$.

$(P\sigma^3/\varepsilon = 0.002\,93$ and $0.004\,82)$. The state points for these calculations are given in the inset of Fig. 4. The nucleation rate increases with temperature along each isobar in accord with intuitive expectation. Again, notice that the rate increases dramatically over a relatively narrow temperature range. More importantly, at fixed temperature the theory predicts that the nucleation rate should increase with decreasing external pressure. This latter trend is remarkable in that the theory is able to capture the correct qualitative behavior at these elevated temperatures without explicitly employing surface tension.

At the thermodynamic spinodal, the free-energy barrier to nucleation must by definition vanish. This indicates that the phase transition mechanism changes from nucleation, an activated process, to spinodal decomposition, a spontaneous one. It is interesting to examine the current kinetic theory is this regard, in particular the connection between the theory and phase stability limits. It should be noted that in reality the transition from metastability to instability occurs smoothly over a region of the metastable portion of the phase diagram,[93–95] the spinodal line being a useful idealization for systems with infinitely long-ranged interactions. By proposing a Ginzburg criterion for nucleation which quantifies the importance of density fluctuations, Binder[94,95] has shown that the width of the transition region from nucleation to spinodal decomposition decreases as the distance to the critical point $(T_c - T)$ increases. The Ginzburg criterion for nucleation states that fluctuations are not important (mean-field theory is accurate) when the mean-squared density fluctuation in the inhomogeneous region separating the nucleus from the bulk fluid is much smaller than the square of the density difference between the liquid and vapor densities. The quantity that measures the relative importance of fluctuations is $\lambda^3(1 - T/T_c)^{1/2}$, where λ is the range of intermolecular interactions in units of the characteristic molecular size. At sufficiently subcritical numbers, when this quantity, the Ginzburg number, is of order unity, the transition region between nucleation and spinodal decomposition is preceded by a ''spinodal nucleation'' region, which defines the region of the phase diagram where the phase transition mechanism is not well-described by classical theory (i.e., at high supersaturation).[93] The initial boundary of this spinodal nucleation region should in fact correspond to the condition that the effective barrier height is of the order k_BT, indicating that ordinary thermal fluctuations are sufficient to trigger the phase transformation. Therefore, the set of state points that satisfies this condition constitutes a kinetically defined spinodal. In Figs. 13 and 14, we show the calculated kinetic spinodal line in the pressure–temperature and temperature–density planes. Notice that at low temperatures, the kinetic spinodal corresponds to a metastability value of approximately 0.5 and therefore lies midway between the thermodynamic binodal and spinodal. At low enough temperatures, the kinetic spinodal precedes the thermodynamic spinodal, and the thermodynamic spinodal can be viewed as the ultimate limit of stability. As temperature increases, the degree of metastability along the kinetic spinodal also increases and approaches a value of unity (i.e., the kinetic spinodal meets the thermodynamic spinodal). For the current version of the

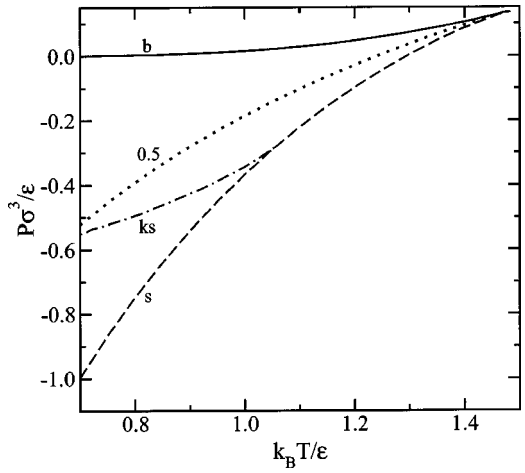

FIG. 13. Kinetic spinodal curve (——) in the pressure–temperature projection of the Lennard-Jones phase diagram. The plotted kinetic spinodal is defined to be the set of points for which the effective free-energy barrier height is of the order k_BT. The binodal (—) and spinodal (– – –) curves are also shown. For reference, line of constant degree of metastability (– – –), $\Delta\mu/\Delta\mu_{spin}=0.5$, is also drawn.

kinetic nucleation theory, based on the assumption that $\rho_V \ll \rho_L$, the kinetic spinodal is predicted to intersect the thermodynamic one at a reduced temperature of $k_BT/\varepsilon=1.055$ $(T/T_c\approx 0.70)$. An alternative criterion for the kinetic spinodal that avoids the calculation of an effective barrier height involves instead the set of points for which $J_{SS}/\beta(0)f(0)=1$. Note that the physical situation that corresponds to this criterion is one where the rate of the phase transformation is comparable to that of single molecule collisions or fluctuations. The kinetic spinodal defined in this way generates a line that is visually indistinguishable from the previously defined kinetic spinodal using the criterion that the barrier height is of order k_BT. That the kinetic spinodal does not extend up to higher temperatures close to the critical point is ascribed to the simplifying assumption in the theory that the density of the vapor is much less than that of the liquid, which becomes invalid at elevated temperatures. In spite of this, at low temperatures, where the kinetic theory is believed to capture the relevant physics of nucleation, the trends are clear: the kinetic spinodal always precedes the thermodynamic one and approaches it with increasing temperature.

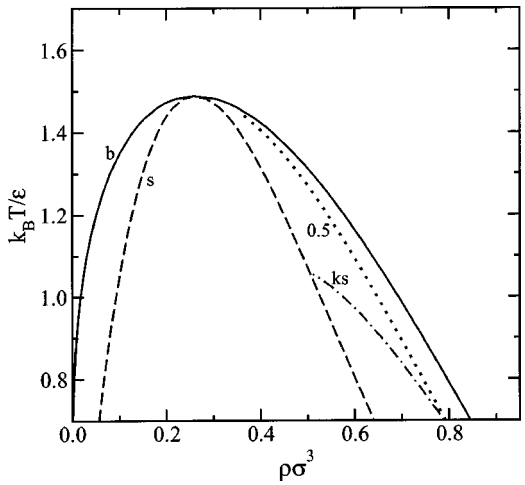

FIG. 14. Kinetic spinodal curve (——) in the pressure–temperature projection of the Lennard-Jones phase diagram. The plotted kinetic spinodal is defined to be the set of points for which the effective free-energy barrier height is of the order k_BT. The binodal (—) and spinodal (– – –) curves are also shown. For reference, line of constant degree of metastability (---), $\Delta\mu/\Delta\mu_{spin}=0.5$, is also drawn.

V. CONCLUSIONS

We have presented a kinetic theory for homogeneous bubble nucleation. The theory is based upon explicit calculation of surface evaporation and condensation rates. The latter is calculated from the kinetic theory of gases, while the former is calculated by exploiting the potential energy minimum in the field established by the interface separating the emerging vapor embryo from the metastable liquid. The surface evaporation rate is directly related to the rate of escape of molecules from the potential-well region. Knowledge of these rates as a function of embryo size allows them to be incorporated directly into a population balance based on the number excess in the emerging bubble. For the Lennard-Jones liquid under isotropic tension, the kinetic theory predicts that the nucleation rate increases with degree of metastability at fixed temperature, while the size of the critical nucleus decreases. Comparison with classical theory also reveals a markedly different metastability dependence of the overall nucleation rate. An important nontrivial prediction made by this theory that classical theory fails to predict is that the nucleation rate increases with decreasing temperature at fixed degree of metastability. For the Lennard-Jones liquid heated above its boiling point, the predicted nucleation rate increases with temperature at fixed external pressure, and also increases with decreasing external pressure at fixed temperature. We have also explored the connection of KNT to phase stability by mapping out kinetically predicted spinodal curves. For the state points explored, the kinetic spinodal always precedes the thermodynamic spinodal, and approaches it with increasing temperature. Finally, an important aspect of this work concerns the observation that the predictions of the kinetic theory follow the thermodynamic scaling relations derived for bubble formation. Although we have used the scaling relations to validate the kinetic theory, the opposite could also be said, namely that the generality of the scaling relations is suggested by the fact that the predictions of an independent kinetics-based theory adhere to them. Extension of these relations to more complex systems such as mixtures can provide a powerful analysis tool, as has been recently suggested by Muller *et al.*[96] in their studies of bubble nucleation in binary polymer solutions.

While the kinetic theory presented in this paper represents a necessary step towards rigorous, kinetics-based treatment of bubble nucleation, there are important aspects of the theory that deserve critical evaluation. An important feature is the assumption that the density of the critical bubble is that of the stable vapor. Density-functional theory has shown that this is only a reasonable assumption up to moderate penetrations into the metastable region. Incorporation of DFT-predicted density profiles for the critical bubble into the calculation of the potential energy field deserves investigation.

A crucial aspect of this theory is the consideration of evaporation and condensation events involving only single molecules. Inclusion of multiple-molecule events, while difficult, should not be disregarded. Molecular dynamics simulations of supercooled vapors have revealed that such events are not completely negligible in the case of droplet nucleation.[78] The relevance of such events to bubble nucleation remains unknown.

Hydrodynamic effects can in principle play a role in the kinetics of bubble formation.[97,98] This is because the growth and shrinkage of embryos occurs in a liquid that possesses nonzero viscosity and is denser than the bubble. This effect, which could prove significant for large enough bubbles, has not been considered in the present theory, and should be the subject of future work.

ACKNOWLEDGMENT

One of the authors P.G.D. gratefully acknowledges the financial support of the U.S. Department of Energy, Division of Chemical Sciences, Geosciences, and Biosciences, Office of Basic Energy Sciences (Grant No. DE-FG02-87ER13714).

APPENDIX A: DISSOCIATION TIME

In this Appendix, we derive the dissociation or escape time of a molecule within the potential well as a function of its initial position, $\tau(r_0;R)$. Let $Q(t|r_0)$ denote the survival probability, that is to say the probability that a molecule initially in the potential well region remains there after time t. Mathematically, it is defined as

$$Q(t|r_0)=\int_{r_{\rm dis}}^{r_b} dr\cdot r^2\cdot p(r,t|r_0) \quad \text{for } r_{\rm dis}<r_0<r_b. \tag{A1}$$

Note that the survival probability has the following properties:

$$Q(0|r_0)=1 \quad \text{for } r_{\rm dis}<r_0<r_b, \tag{A2}$$

and

$$Q(t\to\infty|r_0)=0 \quad \text{for } r_{\rm dis}<r_0<r_b. \tag{A3}$$

Therefore, the probability that a molecule initially located in the potential-well region has escaped between time 0 and t is just $1-Q(t|r_0)$. Thus, the mean escape time as a function of initial position, $\tau(r_0;R)$, is

$$\tau(r_0;R)=\int_0^\infty dt\cdot t\cdot\frac{\partial}{\partial t}[1-Q(t|r_0)]. \tag{A4}$$

Integrating by parts and using the properties of $Q(t|r_0)$, the mean escape time $\tau(r_0;R)$ reduces to

$$\tau(r_0;R)=\int_0^\infty dt\cdot Q(t|r_0). \tag{A5}$$

We now make use of the backward Smoluchowski equation, Eq. (25), by multiplying both sides of it by r^2 and then integrating with respect to r over the potential well region to obtain

$$\frac{\partial}{\partial t}Q(t|r_0)=\frac{D}{r_0^2}\exp\left[\frac{\phi(r_0;R)}{k_BT}\right]\frac{\partial}{\partial r_0}\times\left\{r_0^2\exp\left[\frac{-\phi(r_0;R)}{k_BT}\right]\frac{\partial}{\partial r_0}Q(t|r_0)\right\}. \tag{A6}$$

Finally, integrating both sides with respect to time t from 0 to ∞ yields a differential equation for the mean dissociation time $\tau(r_0;R)$

$$\frac{D}{r_0^2}\exp\left[\frac{\phi(r_0;R)}{k_BT}\right]\frac{d}{dr_0}\left\{r_0^2\exp\left[\frac{-\phi(r_0;R)}{k_BT}\right]\frac{d}{dr_0}\tau(r_0;R)\right\}=-1. \tag{A7}$$

The above differential equation is solved using a ''no flux'' or ''reflective'' boundary condition at $r_0=r_b$

$$\left.\frac{d\tau(r_0;R)}{dr_0}\right|_{r_0=r_b}=0, \tag{A8}$$

which physically restricts molecules from moving directly into the surrounding liquid, and a ''perfect absorption'' boundary condition at $r_0=r_{\rm dis}$

$$\tau(r_0;R)|_{r_0=r_{\rm dis}}=0, \tag{A9}$$

which simply states that molecules beyond $r_{\rm dis}$ are free from the influence of the potential field. Solving Eq. (A7) with the two boundary conditions yields an expression for the mean dissociation time as a function of initial position $\tau(r_0;R)$

$$\tau(r_0;R)=\int_{r_{\rm dis}}^{r_0} dy\cdot\frac{\exp[\phi(y;R)/k_BT]}{y^2}\int_y^{r_b} dx\cdot\frac{x^2}{D}\cdot\exp\left[\frac{-\phi(x;R)}{k_BT}\right]. \tag{A10}$$

APPENDIX B: SCALING RELATIONS

In this Appendix, we reproduce the key steps in deriving the scaling relations given in Eqs. (36) and (37). To this end, it is postulated that the relationship between the free-energy barrier height, W^*, the nominal thermodynamic driving force. $\Delta\mu$, and the number excess in the critical embryo, Δn^*, can be written in the following form:

$$\frac{W^*}{\Delta\mu\cdot\Delta n^*}=\frac{1}{2}-h(\Delta n^*,\Delta\mu), \tag{B1}$$

where the unknown function $h(\Delta n^*,\Delta\mu)$ describes the departure from classical behavior. Note that $h=0$ corresponds to agreement with classical nucleation theory. Differentiating this equation with respect to $\Delta\mu$ at constant temperature and using the nucleation theorem, Eq. (35), yields the following differential equation:

$$3\Delta n^*+\Delta\mu\cdot\frac{d}{d\Delta\mu}\Delta n^*=2\frac{d}{d\Delta\mu}[\Delta\mu\cdot\Delta n^*\cdot h(\Delta n^*,\Delta\mu)]. \tag{B2}$$

Because $h(\Delta n^*, \Delta\mu)$ is unknown, it is assumed that each side of the above equation vanishes identically, and therefore each side can be solved separately for Δn^* and $h(\Delta n^*, \Delta\mu)$, yielding

$$\Delta n^* = C(T) \cdot (\Delta\mu)^{-3}, \tag{B3}$$

and

$$\Delta n^* \cdot h(\Delta n^*, \Delta\mu) = D(T) \cdot (\Delta\mu)^{-1}, \tag{B4}$$

where $C(T)$ and $D(T)$ are temperature-dependent constants of integration. Note that Eq. (B3) is precisely the scaling relation given in Eq. (36). Substitution of Eqs. (B3) and (B4) into Eq. (B1) yields the second scaling relation given in Eq. (37).

[1] P. G. Debenedetti, *Metastable Liquids: Concepts and Principles* (Princeton University Press, Princeton, N.J., 1996).
[2] D. H. Trevena, *Cavitation and Tension in Liquids* (Hilger, Bristol, England; Philadelphia, 1987).
[3] R. C. Reid, Science **203**, 1265 (1979).
[4] D. Kivelson and H. Reiss, J. Phys. Chem. B **103**, 8337 (1999).
[5] D. S. Corti and P. G. Debenedetti, Chem. Eng. Sci. **49**, 2717 (1994).
[6] D. S. Corti and P. G. Debenedetti, Ind. Eng. Chem. Res. **34**, 3573 (1995).
[7] F. H. Stillinger, Phys. Rev. E **52**, 4685 (1995).
[8] D. S. Corti, P. G. Debenedetti, S. Sastry, and F. H. Stillinger, Phys. Rev. E **55**, 5522 (1997).
[9] P. A. Lush, J. Fluid Mech. **135**, 373 (1983).
[10] Y. L. Chen and J. Israelachvili, Science **252**, 1157 (1991).
[11] M. Shusser and D. Weihs, Int. J. Multiphase Flow **25**, 1561 (1999).
[12] H. Y. Kwak and R. L. Panton, J. Phys. D **18**, 647 (1985).
[13] S. J. Putterman, Sci. Am. **272**, 46 (1995).
[14] K. S. Suslick, Science **247**, 1439 (1990).
[15] C. T. Avedisian, J. Phys. Chem. Ref. Data **14**, 695 (1985).
[16] R. C. Reid, Am. Sci. **64**, 146 (1976).
[17] G. D. N. Overton, P. R. Williams, and D. H. Trevena, J. Phys. D **17**, 979 (1984).
[18] D. D. Joseph, J. Fluid Mech. **366**, 367 (1998).
[19] B. Nowakowski and E. Ruckenstein, J. Colloid Interface Sci. **139**, 500 (1990).
[20] E. Ruckenstein and B. Nowakowski, J. Colloid Interface Sci. **137**, 583 (1990).
[21] E. Ruckenstein and B. Nowakowski, Langmuir **7**, 1537 (1991).
[22] B. Nowakowski and E. Ruckenstein, J. Chem. Phys. **94**, 8487 (1991).
[23] B. Nowakowski and E. Ruckenstein, J. Colloid Interface Sci. **142**, 599 (1991).
[24] B. Nowakowski and E. Ruckenstein, J. Chem. Phys. **94**, 1397 (1991).
[25] B. Nowakowski and E. Ruckenstein, J. Phys. Chem. **96**, 2313 (1992).
[26] G. Narsimhan and E. Ruckenstein, J. Colloid Interface Sci. **128**, 549 (1989).
[27] R. McGraw and A. Laaksonen, Phys. Rev. Lett. **76**, 2754 (1996).
[28] V. K. Shen and P. G. Debenedetti, J. Chem. Phys. **114**, 4149 (2001).
[29] M. Berthelot, Ann. Chim. Phys. **30**, 232 (1850).
[30] M. Blander and J. L. Katz, J. Stat. Phys. **4**, 55 (1972).
[31] M. Blander and J. L. Katz, AIChE J. **21**, 833 (1975).
[32] F. H. Stillinger, J. Chem. Phys. **38**, 1486 (1963).
[33] I. Kusaka and D. W. Oxtoby, J. Chem. Phys. **110**, 5249 (1999).
[34] P. Schaaf, B. Senger, J. C. Voegel, and H. Reiss, Phys. Rev. E **60**, 771 (1999).
[35] P. R. ten Wolde, M. J. Ruizmontero, and D. Frenkel, Phys. Rev. Lett. **75**, 2714 (1995).
[36] S. Auer and D. Frenkel, Nature (London) **409**, 1020 (2001).
[37] J. X. Zhu, M. Li, R. Rogers, W. Meyer, R. H. Ottewill, W. B. Russell, and P. M. Chaikin, Nature (London) **387**, 883 (1997).
[38] P. N. Pusey, W. Vanmegen, P. Bartlett, B. J. Ackerson, J. G. Rarity, and S. M. Underwood, Phys. Rev. Lett. **63**, 2753 (1989).
[39] P. R. ten Wolde and D. Chandler, Proc. Natl. Acad. Sci. U.S.A. **99**, 6539 (2002).
[40] K. Lum, D. Chandler, and J. D. Weeks, J. Phys. Chem. B **103**, 4570 (1999).
[41] D. M. Huang and D. Chandler, Phys. Rev. E **61**, 1501 (2000).
[42] D. M. Huang, P. L. Geissler, and D. Chandler, J. Phys. Chem. B **105**, 6704 (2001).
[43] D. Chandler, Nature (London) **417**, 491 (2002).
[44] S. Punnathanam and D. S. Corti, Ind. Eng. Chem. Res. **41**, 1113 (2002).
[45] N. R. Kestner, J. Jortner, M. H. Cohen, and S. A. Rice, Phys. Rev. **140**, A56 (1965).
[46] C. M. Surko and F. Reif, Phys. Rev. **175**, 229 (1968).
[47] A. D. J. Haymet and D. W. Oxtoby, J. Chem. Phys. **74**, 2559 (1981).
[48] P. Harrowell and D. W. Oxtoby, J. Chem. Phys. **80**, 1639 (1984).
[49] D. W. Oxtoby and R. Evans, J. Chem. Phys. **89**, 7521 (1988).
[50] X. C. Zeng and D. W. Oxtoby, J. Chem. Phys. **94**, 4472 (1991).
[51] C. K. Bagdassarian and D. W. Oxtoby, J. Chem. Phys. **100**, 2139 (1994).
[52] Y. C. Shen and D. W. Oxtoby, J. Chem. Phys. **104**, 4233 (1996).
[53] A. Laaksonen and D. W. Oxtoby, J. Chem. Phys. **102**, 5803 (1995).
[54] X. C. Zeng, D. W. Oxtoby, and E. Cheng, J. Chem. Phys. **104**, 3726 (1996).
[55] L. A. Baez and P. Clancy, J. Chem. Phys. **102**, 8138 (1995).
[56] S. Park, J. G. Weng, and C. L. Tien, Microscale Thermophys. Eng. **4**, 161 (2000).
[57] S. H. Park, J. G. Weng, and C. L. Tien, Int. J. Heat Mass Transf. **44**, 1849 (2001).
[58] M. Matsumoto, S. Saito, and I. Ohmine, Nature (London) **416**, 409 (2002).
[59] S. C. Gay, E. J. Smith, and A. D. J. Haymet, J. Chem. Phys. **116**, 8876 (2002).
[60] N. Waheed, M. S. Lavine, and G. C. Rutledge, J. Chem. Phys. **116**, 2301 (2002).
[61] K. Laasonen, S. Wonczak, R. Strey, and A. Laaksonen, J. Chem. Phys. **113**, 9741 (2000).
[62] S. Toxvaerd, J. Chem. Phys. **115**, 8913 (2001).
[63] T. Kinjo and M. Matsumoto, Fluid Phase Equilib. **144**, 343 (1998).
[64] B. Chen, J. I. Siepmann, K. J. Oh, and M. L. Klein, J. Chem. Phys. **116**, 4317 (2002).
[65] B. Chen, J. I. Siepmann, K. J. Oh, and M. L. Klein, J. Chem. Phys. **115**, 10903 (2001).
[66] P. R. ten Wolde, D. W. Oxtoby, and D. Frenkel, Phys. Rev. Lett. **81**, 3695 (1998).
[67] P. R. ten Wolde, D. W. Oxtoby, and D. Frenkel, J. Chem. Phys. **111**, 4762 (1999).
[68] I. Kusaka, Z. G. Wang, and J. H. Seinfeld, J. Chem. Phys. **108**, 3416 (1998).
[69] J. S. Vanduijneveldt and D. Frenkel, J. Chem. Phys. **96**, 4655 (1992).
[70] P. R. ten Wolde, M. J. RuizMontero, and D. Frenkel, Faraday Discuss. **104**, 93 (1996).
[71] P. R. ten Wolde, M. J. RuizMontero, and D. Frenkel, J. Chem. Phys. **104**, 9932 (1996).
[72] V. K. Shen and P. G. Debenedetti, J. Chem. Phys. **111**, 3581 (1999).
[73] I. Kusaka and D. W. Oxtoby, J. Chem. Phys. **111**, 1104 (1999).
[74] D. W. Oxtoby and D. Kashchiev, J. Chem. Phys. **100**, 7665 (1994).
[75] R. K. Bowles, R. McGraw, P. Schaaf, B. Senger, J. C. Voegel, and H. Reiss, J. Chem. Phys. **113**, 4524 (2000).
[76] R. K. Bowles, D. Reguera, Y. Djikaev, and H. Reiss, J. Chem. Phys. **115**, 1853 (2001).
[77] V. Talanquer, J. Chem. Phys. **106**, 9957 (1997).
[78] P. Schaaf, B. Senger, J. C. Voegel, R. K. Bowles, and H. Reiss, J. Chem. Phys. **114**, 8091 (2001).
[79] G. K. Schenter, S. M. Kathmann, and B. C. Garrett, J. Chem. Phys. **110**, 7951 (1999).
[80] G. K. Schenter, S. M. Kathmann, and B. C. Garrett, Phys. Rev. Lett. **82**, 3484 (1999).
[81] N. M. Dixit and C. F. Zukoski, Phys. Rev. E **64**, 041604 (2001).
[82] B. Shizgal and J. C. Barrett, J. Chem. Phys. **91**, 6505 (1989).
[83] J. Frenkel, *Kinetic Theory of Liquids* (Clarendon, Oxford, 1946).
[84] J. S. Rowlinson and B. Widom, *Molecular Theory of Capillarity* (Oxford, Oxfordshire, 1982).
[85] F. F. Abraham, *Homogeneous Nucleation Theory; The Pretransition Theory of Vapor Condensation* (Academic, New York, 1974).
[86] S. Chandrasekhar, Rev. Mod. Phys. **15**, 1 (1943).
[87] N. Agmon, J. Chem. Phys. **81**, 3644 (1984).
[88] C. W. Gardiner, *Handbook of Stochastic Methods for Physics, Chemistry, and the Natural Sciences*, 2nd ed. (Springer, Berlin; New York, 1990).
[89] J. D. Weeks, D. Chandler, and H. C. Andersen, J. Chem. Phys. **54**, 5237 (1971).
[90] K. Nishioka, Phys. Rev. E **52**, 3263 (1995).

[91] V. P. Skripov, *Metastable Liquids* (Wiley, New York, 1973).
[92] V. G. Baidakov and V. P. Skripov, Exp. Therm. Fluid Sci. **5**, 664 (1992).
[93] C. Unger and W. Klein, Phys. Rev. B **29**, 2698 (1984).
[94] K. Binder, Phys. Rev. A **29**, 341 (1984).
[95] K. Binder, Physica A **140**, 35 (1986).
[96] M. Muller, L. G. MacDowell, P. Virnau, and K. Binder, J. Chem. Phys. **117**, 5480 (2002).
[97] Y. Kagan, J. Phys. Chem. **34**, 42 (1960).
[98] C. E. Brennen, *Cavitation and Bubble Dynamics* (Oxford University Press, Oxford, 1996).